Hindawi
Journal of Robotics
Volume 2024, Article ID 9863834, 1 page
https://doi.org/10.1155/2024/9863834

Retraction

Retracted: Optimization of Intelligent Distribution of Distribution Network in the Presence of Distributed Sources

Journal of Robotics

Received 23 January 2024; Accepted 23 January 2024; Published 24 January 2024

This article has been retracted by Hindawi following an investigation undertaken by the publisher [1]. This investigation has uncovered evidence of one or more of the following indicators of systematic manipulation of the publication process:

(1) Discrepancies in scope
(2) Discrepancies in the description of the research reported
(3) Discrepancies between the availability of data and the research described
(4) Inappropriate citations
(5) Incoherent, meaningless and/or irrelevant content included in the article
(6) Manipulated or compromised peer review

The presence of these indicators undermines our confidence in the integrity of the article's content and we cannot, therefore, vouch for its reliability. Please note that this notice is intended solely to alert readers that the content of this article is unreliable. We have not investigated whether authors were aware of or involved in the systematic manipulation of the publication process.

Wiley and Hindawi regrets that the usual quality checks did not identify these issues before publication and have since put additional measures in place to safeguard research integrity.

We wish to credit our own Research Integrity and Research Publishing teams and anonymous and named external researchers and research integrity experts for contributing to this investigation.

The corresponding author, as the representative of all authors, has been given the opportunity to register their agreement or disagreement to this retraction. We have kept a record of any response received.

References

[1] Y. Song, D. Nie, and L. Fan, "Optimization of Intelligent Distribution of Distribution Network in the Presence of Distributed Sources," *Journal of Robotics*, vol. 2022, Article ID 7063913, 11 pages, 2022.

Hindawi
Journal of Robotics
Volume 2022, Article ID 7063913, 11 pages
https://doi.org/10.1155/2022/7063913

Research Article

Optimization of Intelligent Distribution of Distribution Network in the Presence of Distributed Sources

Youle Song, Ding Nie, and Litao Fan

Yunnan Power Grid Co., Ltd., Electric Power Research Institute, Kunming, Yunnan 650000, China

Correspondence should be addressed to Youle Song; 13648806353@163.com

Received 27 July 2022; Revised 29 August 2022; Accepted 30 August 2022; Published 26 September 2022

Academic Editor: Shahid Hussain

In order to improve the intelligent distribution effect of the distribution network in the presence of distributed generation, this study combines intelligent algorithms to analyze the intelligent distribution of the distribution network in the presence of distributed generation. Moreover, this study establishes an objective function composed of system network loss expectation, voltage stability index, and reactive power compensation equipment investment. In addition, this study improves the artificial bee colony algorithm through tabu search algorithm and genetic algorithm and obtains an improved TS-IABC algorithm. Finally, this study compares and tests the performance of different algorithms in the form of functions and simulations. The simulation results show that the optimal intelligent distribution method of the distribution network in the presence of distributed power generation proposed in this study has a good effect and can promote the intelligent distribution of the distribution network.

1. Introduction

At present, distributed power generation has been developed very rapidly. However, when distributed power sources are used in the distribution network, the structure of the distribution network changes accordingly. The distributed power supply connected to the distribution network can replace the traditional energy system to supply power for the distribution network, which makes the distribution network transform into a multi-power supply system and changes the power flow distribution in the distribution network. Moreover, with the development of distribution network automation technology, various optimization methods and optimization objectives have gradually become the focus of distribution network reconfiguration research. For example, the multi-objective particle swarm algorithm is used to solve the model of distribution network optimization and reconstruction [1], and the radiation network generation algorithm is used to obtain the topology structure that satisfies the radial grid constraints of the distribution network [2]. Distribution network reconfiguration usually refers to changing the operating state of tie switches and segment switches under the condition of satisfying the radial constraints of the distribution network and changing the topology of the distribution network as needed. The reconfiguration model of the distribution network can be divided into static reconfiguration and dynamic reconfiguration model. In the static reconfiguration model, the load demand and power output are assumed to be constant values, while in the dynamic reconfiguration these values are time varying [3].

Power distribution systems are usually configured in a radial fashion, but the action of opening or closing switches or protective relays can change the topology of these systems. Network reconfiguration of a distribution network refers to the concept of closing and opening connection switches without losing the radial structure of the existing distribution network [4]. The complexity of the existing distribution network is becoming more and more complex due to the gradual increase in electricity demand and changes in load. By reconfiguring the network, reducing line losses, and improving system reliability, efficient operation of the distribution network can be achieved. Due to the increased demand for electricity and the high cost of new power plants and transmission lines, the use of distributed power has attracted widespread attention. The benefits of

distributed power sources include increased reliability, improved system fault resilience, and improved voltage conditions. At present, the proportion of distributed power as a supplement to primary energy in various energy sources is gradually increasing [5]. Therefore, the problem of distribution network reconfiguration has also become the research focus of scholars at home and abroad. Literature [6] considered the randomness of wind power output, established a mathematical model with the goal of minimizing network loss and used Wasserstein distance to describe the similarity of wind power scenario models. Literature [7] considers the timing of the fan output and reduces the operating cost of the system through the dynamic reconfiguration strategy of the distribution network. Literature [8] established a model with the goal of minimizing the network loss of the distribution network and considered the uncertainty of the output of wind turbines and photovoltaics to evaluate the reconfiguration value of the distribution network in each time period. Literature [9] comprehensively considers the influence of the uncertainty of wind turbines, photovoltaics, and loads on the distribution network, first forms multiple scenarios, and then uses the EMD distance to evaluate the similarity between the scenarios to reduce the scenarios. Literature [10] considers the uncertainty between the outputs of various distributed power sources and uses a weighted hybrid two-dimensional Copula model to deal with the correlation between the two power sources of wind and solar to establish its probability joint density function to reconstruct the distribution network. Literature [11] is based on the theory that there is a strong correlation between wind speeds and solar irradiance between adjacent positions in the same wind belt and the same radiation belt in the distribution network and considers the correlation between wind speed and irradiance intensity based on Nataf transformation. It is necessary to reconstruct the distribution network with distributed power generation. Literature [12] comprehensively considered the timing of load demand in the distribution network and the uncertainty of photovoltaic output and improved the photovoltaic power consumption through the optimization and reconstruction of the distribution network. In literature [13], the new three-dimensional group search method is applied to the configuration research of distributed power generation, and the purpose of reducing the system network loss is achieved by reconfiguring the distribution network.

The basic idea of the direct algorithm is to combine the topology structure of the distribution network with the graph theory and cooperate with the fault indicator or the fault current information uploaded by the FTU to achieve an accurate fault location. The shortcomings of the direct algorithm are obvious: the actual situation of the distribution network is relatively complex, resulting in a low fault tolerance of the direct algorithm; but the advantages of the algorithm are also very prominent: the principle is simple, and it is widely used in simple distribution networks, and only needs to be used in fault location identification. It can be obtained by calculating the network description matrix and fault information matrix [14]. Literature [15] takes the distribution network feeder as the edge of the graph, and the feeder circuit breaker and the recloser as the graph nodes to form a fault information matrix and a network description matrix, and then proposes a method that can shorten the fault location identification and isolation. A new algorithm—branch-node distribution network fault location identification algorithm. In literature [16], considering the direction of the fault current, in order to realize the fault location identification of a radial network, tree network, and ring network, an improved matrix algorithm is proposed. However, this improved algorithm is only suitable for a single fault. To solve the problem of terminal faults and multiple faults on different lines, literature [17] proposes an improved matrix algorithm and proposes an executable standard to realize fault location identification. Literature [18] proposed an improved method, adding zero node numbers at the ends of radial networks and tree networks to eliminate blind spots and realize fault location identification. Literature [19] proposed an improved matrix algorithm for fault cross-sectional location in the distribution network. According to the FTU communication status or fault indication signal and the distribution network topology, the attribute matrix is constructed, and the network description matrix information is dynamically established to identify the fault location of the distribution network [20] regards the distribution network as a tree diagram and uses the adjacency matrix method to realize the processing of the graph, thereby proposing an algorithm for identifying the fault location of overheated arcs. The arc conversion method has achieved good results in the field of distribution network fault location. Literature [21] proposed a fault location determination algorithm based on topology identification, considering the location of the T node of the distribution network. The algorithm fully considers the characteristics of distribution network fault location, so it can effectively judge the fault part of distribution network, automatically determine the nodes in the area, and adapt to the changes of network structure.

This study combines the intelligent algorithm to analyze the optimization of the intelligent distribution of the distribution network in the presence of distributed power generation and improves the intelligent analysis and reconstruction effect of the distribution network.

2. Intelligent Distribution Algorithm of Distribution Network

The design of the distribution network is mostly based on closed-loop design and open-loop operation. The open-loop system has many advantages, such as a small short-circuit current, simple protection and control, easy fault diagnosis and isolation, convenient service, and a small breaking current. Before the reconfiguration of the distribution network, the topology should be transformed into a radial network structure.

In this study, network reconstruction is carried out before reactive power optimization. The basic idea is as follows: all the reconstructed network topologies are searched and numbered ([1,2,3,...,n], where n is the number of topological structures). The number of reconstructions is

the same as the number of numbers, and the topology number is used as a control variable in the optimization process. Therefore, the reactive power optimization after reconstruction only adds one control variable to the original model.

This study combines the knowledge of graph theory in circuit analysis to find all the topologies after reconstruction. All switches in the distribution network are closed to form a connectivity graph, and the radial network operates as a tree in the connectivity graph, which is the same as the reconfigured distribution network. Therefore, the set of all trees in the connected graph is the set of all the results produced by the reconstruction.

If the connected graph of the n-node system has b branches, the tree set is calculated as: n nodes correspond to (n−1) tree branches, and all combinations of (n−1) branches are selected from all branches. After the combinations that cannot form a tree are deleted, what remains is all the tree sets of the connected graph.

The process of distribution network reconstruction can be carried out before reactive power optimization, and only one reconstruction can be performed for a specific network, which does not affect the speed of the model solution in the process of reactive power optimization.

Scientific and technological progress has promoted the effective use of natural resources such as solar energy and wind energy. The establishment of photovoltaic power stations and the installation of wind power generation systems have increased the grid-connected penetration rate of distributed power sources, which has brought corresponding problems while reducing power generation costs. The uncertainty of DG output is greatly affected by the environment, and the impact on the power grid cannot be underestimated. At the same time, with the progress of industrial development, new loads with fluctuating (electric arc furnace, electric welding machine, and other smelting loads) and impact (rolling mills, cranes, etc.) are generated. Its power situation is greatly affected by the load situation, and it is difficult to replace it with a certain value, and its influence cannot be ignored. Combined with the analysis and probability constraints of DG in Chapters 2 and 3, a static reactive power optimization model is established, which can be expressed as follows:

$$\begin{cases} \min f(X,\xi), \\ g(X,\xi) = 0, \\ \Pr\left(\xi_{\min} \le \xi \le \xi_{\max}\right) \ge \beta, \\ X_{\min} \le X \le X_{\max}. \end{cases} \tag{1}$$

Among them, $f(X,\xi)$ is the objective function and X is the control variable. There are discrete variables such as the topology of the distribution network system, the number of capacitor banks, and OLTC tap positions, and there are continuous variables such as static reactive power compensator (SVG) and generator terminal voltage. At the same time, $X_{\min}, X_{\max}$ are the upper and lower limits of the control variable, $\xi_{\min}, \xi_{\max}$ are the upper and lower limits of the state variable, and $\Pr(*)$ is the probability of reaching the event. β is the confidence level of the state variable and $g(X,\xi) = 0$ is the equality constraint.

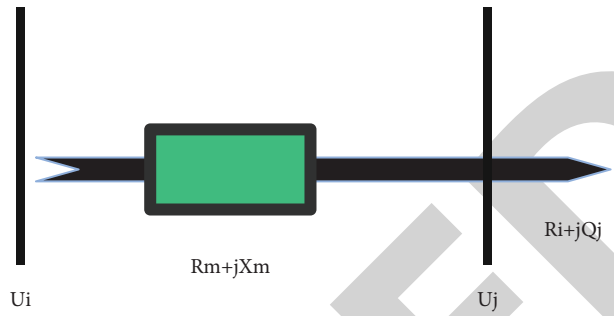

Figure 1: Equivalent circuit of distribution network.

The safety and economy of the power distribution system are considered. This study establishes a multi-objective function with the minimum static voltage stability index, the minimum expected system active power loss, and the minimum investment in reactive power compensation equipment.

2.1. Static Voltage Stability Index of Distribution Network. The magnitude of the voltage stability index reflects the voltage stability of the power system. Too high system voltage will damage electrical equipment and insulation, and too low voltage will affect the normal operation of equipment, and even cause system collapse, resulting in serious consequences.

Figure 1 shows a selected branch, the branch nodes are i and j respectively, and the flow direction is set from i to j.

Any branch has

$$\begin{cases} P_i = \dfrac{\left(P_i^2 + Q_t^2\right)R}{U_i^2} + P_j, \\ Q_i = \dfrac{\left(P_i^2 + Q_i^2\right)X}{U_i^2} + Q_j. \end{cases} \tag{2}$$

In the formula, P_i is the active and reactive power of Q_i at node i, P_j, Q_j is the active and reactive power of node j, respectively, R and X are the resistance and reactance of branch ij, respectively. If the active and reactive power of node i is taken as the independent variable, the conditions for (2) to have a real number solution are

$$\frac{4\left(XP_j - RQ_j\right)^2 + \left(XQ_j - RP_j\right)U_i^2}{U_i^4} < 1. \tag{3}$$

If the per unit value of the terminal voltage is taken as 1.0, there is

$$4\left(XP_j - RQ_j\right)^2 + XQ_j + RP_j < 1. \tag{4}$$

Therefore, the voltage stability index can be defined as follows:

$$L = 4\left(XP_j - RQ_j\right)^2 + XQ_j + RP_j. \tag{5}$$

The smaller the distance between L and 1, the worse the voltage quality. The greater the distance from 1, the better the voltage quality. The closer L is to 1, the closer the system is to collapse. The maximum value of L in the system is used as the voltage stability index of the whole system, that is,

$$L_{\max} = \max\left(L_1, L_2, \ldots, L_{N-1}\right). \tag{6}$$

In the formula, N is the number of system nodes. $L_{\max}$ corresponds to the weakest branch. If the system crashes, it must happen at $L_{\max}$.

2.2. System Network Loss Expectations. The system network loss and its expectation can be expressed as follows:

$$E\left(P_{\text{loss}}\right) \approx \sum_{k=1}^{n} \sum_{m=1}^{3} P_{xk,m} P_{\text{loss}}(k,m), \tag{7}$$

$$P_{\text{Loss}} = \sum_{i=1}^{N} \sum_{j \in \Theta_i} \tau_{ij} g_{ij}\left(u_i^2 + u_j^2 - 2u_i u_j \cos\,\theta_{ij}\right). \tag{8}$$

Among them, N is the total number of system nodes, i and j are node labels, and Θ_i is the set of nodes adjacent to node i. At the same time, τ_{ij} is the on–off state of the branch ij, $\tau_{ij} = 0$ represents the open circuit, and $\tau_{ij} = 1$ represents the channel. g_{ij} is the branch admittance between nodes i and j, θ_{ij} is the phase angle difference between nodes i and j, and u_i, u_j are the voltage amplitude of the corresponding node, respectively.

(3) With the expansion of the scale of the power system and the rapid evolution of the power market, the pricing system of the electricity price has been continuously improved, which makes the pricing system of the reactive power price more reasonable and perfect. Therefore, the reactive power optimization should reasonably choose the optimization target according to the actual situation. The optimization objective of this study increases the minimum investment of reactive power compensation equipment, which can be expressed as follows:

$$\min F = \min \sum_{s \in N_c} C_{CAP_s} \left| Q_{qs} \right|. \tag{9}$$

Among them, $s \in N_C$ represents that the reactive power compensation equipment is adjusted at node s, and C_{CAPP_s} and Q_{qs} represent the unit capacity cost of the s node equipment and the actual reactive power compensation capacity at this point.

(1) Power flow constraints:

$$\begin{cases} \Delta P_i = P_{is} - \sum_{g \in i} V_i V_g\left(G_{ig} \cos\,\theta_{ig} + B_{ig} \sin\,\theta_{ig}\right) = 0, \\ \Delta Q_i = Q_{is} - \sum_{g \in i}^{N} V_i V_g\left(G_{ig} \sin\,\theta_{ig} - B_{ig} \cos\,\theta_{ig}\right) = 0. \end{cases} \tag{10}$$

In the formula, the total number of system nodes is $N; i = 1, 2, \ldots, N; G_{ig}, B_{ig}$, and θ_{ig} are the admittance and phase angle difference between nodes i and g, respectively. At the same time, $g \in i$ is the node connected to node i, V_i and V_g are the voltage amplitude of the corresponding node, P_{is} and Q_{is} are the active and reactive power injected by the corresponding node, respectively. If the power out of bounds occurs in the optimization process, the calculation is performed according to the corresponding boundary value.

(2) Inequality constraints:

$$\begin{cases} \Pr\left(V_{i,\min} \le V_i \le V_{i,\max}\right) \ge \beta, \\ Q_{SVC,i,\min} \le Q_{SVC,i} \le Q_{SVC,i,\max}, \\ T_{\min} \le T \le T_{\max}, \\ Q_{Ci,\min} \le Q_{C_i} \le Q_{C_i,\max}, \\ P_{DG,\min} \le P_{DG,i} \le P_{DG,\max}, \\ Q_{DG,\min} \le Q_{DG,i} \le Q_{DG,\max}, \\ g_k \in G. \end{cases} \tag{11}$$

In the formula, $\Pr(*)$ is the probability of event achievement, β is the confidence level of the state variable, and $V_{i,\min}$ and $V_{i,\max}$ are the minimum and maximum voltage of node i, respectively. T, $T_{\min}$, and $T_{\max}$ are the gear position and extreme value of the on-load voltage regulating transformer, respectively, and Q_{C_i} and $Q_{C_i,\min}, Q_{C_i,\max}$ are the capacity and extreme value of the capacitor installed at node i, respectively. At the same time, $P_{DG,i}, P_{DG,\min}, P_{DG,\max}$, $Q_{DG,\min}$, and $Q_{DG,\max}$ are the capacity and extreme value of the active and reactive power connected to the DG at node i, respectively, $Q_{SVC,i}, Q_{SVC,i,\min}$, and $Q_{SVC,i,\max}$ are the compensation capacity and extreme value of the SVG, respectively, and g_k and G is the topology and feasible topology set after network reconstruction, respectively.

2.3. Penalty Function of Voltage Exceeding Limit. In order to solve the situation that some node voltages do not meet the conditions, the probability constraints of node voltages are embedded into the objective function in the form of penalty functions, such as

$$V(v) = a_3 \sum_{i=1}^{N} P\left(v_i\right). \tag{12}$$

Among them, a_3 is the coefficient of the penalty function, and $P(v_i)$ can be expressed as

$$P\left(v_i\right) = \begin{cases} \beta - \Pr\left(v_{i,\min} \le v_i \le v_{i,\max}\right), \Pr\left(v_{i,\min} \le v_i \le v_{i,\max}\right) < \beta, \\ 0, \Pr\left(v_{i,\min} \le v_i \le v_{i,\max}\right) \ge \beta. \end{cases} \tag{13}$$

The Artificial Bee Colony Algorithm (ABC) stipulates that there is at most one scout bee, and the number of lead bees and observer bees is equal. There is a one-to-one relationship between the lead bee and the nectar source. If the amount of honey at the location of the nectar source is insufficient due to multiple collections, the lead bee will

change its role to a scout bee, research in the neighborhood, and randomly generate a new nectar source. The transformation of the role of the bee is shown in Figure 2.

The steps to implement the artificial bee colony algorithm are

(1) The initial parameters are set. The total number of bee colonies is set to N, each nectar source searches Limit times at most, and the system circulates MCN times at most.

(2) The population is initialized. The lead bee randomly generates a new initial solution according to formula (1).

$$x_i^{'j} = x_i^j + \text{rand}\left(x_i^j - x_k^j\right). \tag{14}$$

(i) Among them, x_i^j is the solution of dimension j in nectar i, there is $i, k \in \{1, 2, \ldots, SN\}$ and $i \neq k$, $j \in \{1, 2, \ldots, D\}$. rand takes a random number between $[-1, 1]$. D is the optimization parameter, and all solutions are D-dimensional vectors.

(3) The lead bee searches the neighborhood according to formula (15) to generate a new solution.

$$x_{i,\text{new}} = x_{\min} + \text{rand}\,(0, 1)\left(x_{\max} - x_{\min}\right). \tag{15}$$

(4) The fitness function (16) is calculated, the searched new nectar source is compared with the old nectar source, and the one with a higher fitness function is selected.

The fitness function can be expressed as:

$$\text{fit}_i = \begin{cases} \dfrac{1}{1 + f\left(x_i\right)}, & f\left(x_i\right) > 0, \\ 1 + \left|f\left(x_i\right)\right|, & f\left(x_i\right) < 0. \end{cases} \tag{16}$$

(i) Among them, $f(x_i)$ is the objective function value corresponding to the solution x_i.

(5) According to formula (17), the following probability P_i is obtained:

$$P_i = \frac{\text{fit}\left(X_i\right)}{\sum_{i=1}^{N} \text{fit}\left(X_i\right)}. \tag{17}$$

(i) Among them, P_i is the probability that the nectar source i is selected by the observer bees, and $\text{fit}(X_i)$ is the fitness function value of the nectar source i.

(6) Observer bees are transformed into lead bees according to P_i to conduct spatial search and update the nectar source.

(7) If a single nectar source reaches the maximum number of searches Limit, but it is not updated, formula (8) is performed. Otherwise, it goes to formula (9).

(8) The lead bees turn into scout queens to search for new nectar sources globally and replace the old nectar sources.

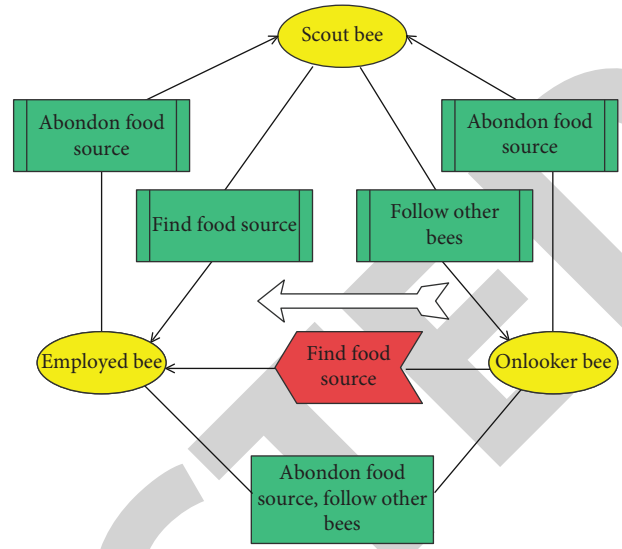

Figure 2: Mutual conversion of bee roles.

(9) The obtained optimal solution is saved.

(10) If the maximum number of cycles MCN is reached, formula (11) is entered, otherwise, it returns to formula (3). The loop of formula (11) ends. The optimal solution at this time is the global optimal solution, and the corresponding nectar source is the minimum value of the sought function. The flow chart is shown in Figure 3.

Tabu search algorithm is often used to search for the global optimum. In the algorithm, in order to achieve global optimization, a storage structure is introduced to store relevant data in the memory search process, which can provide guidance for subsequent searches. We avoid repeated searches for the same target during the search process by formulating taboo criteria. In order to ensure the diversity of the search, the contempt criterion is used to absolve the excellent individuals who are forbidden in the search process, so as to achieve global optimization. Its algorithm flowchart is shown in Figure 4.

Due to the poor search ability of the traditional artificial bee colony algorithm, Zhu and Kwong improved the traditional algorithm to improve the performance of the algorithm. The global best is added to formula (14) to form the Gbest-guided artificial bee colony algorithm (GABC). The modified expression (18) is

$$x_i^{'j} = x_i^j + \text{rand}\left(x_i^j - x_k^j\right) + \beta\left(x_{\text{Global}}^j - x_i^j\right). \tag{18}$$

The convergence speed of the algorithm is improved by $\beta(x_{\text{Global}}^j - x_i^j)$, but the global optimization ability cannot be improved. Therefore, an Improved Artificial Bee Colony Algorithm (IABC) is obtained by introducing the binomial crossover operation in the genetic algorithm. In the binomial crossover method, each component randomly generates a rand between [0, 1]. When there is $\text{rand} < cr$ (cr is the set value), the target component is accepted. Otherwise, the corresponding component of the current individual remains unchanged.

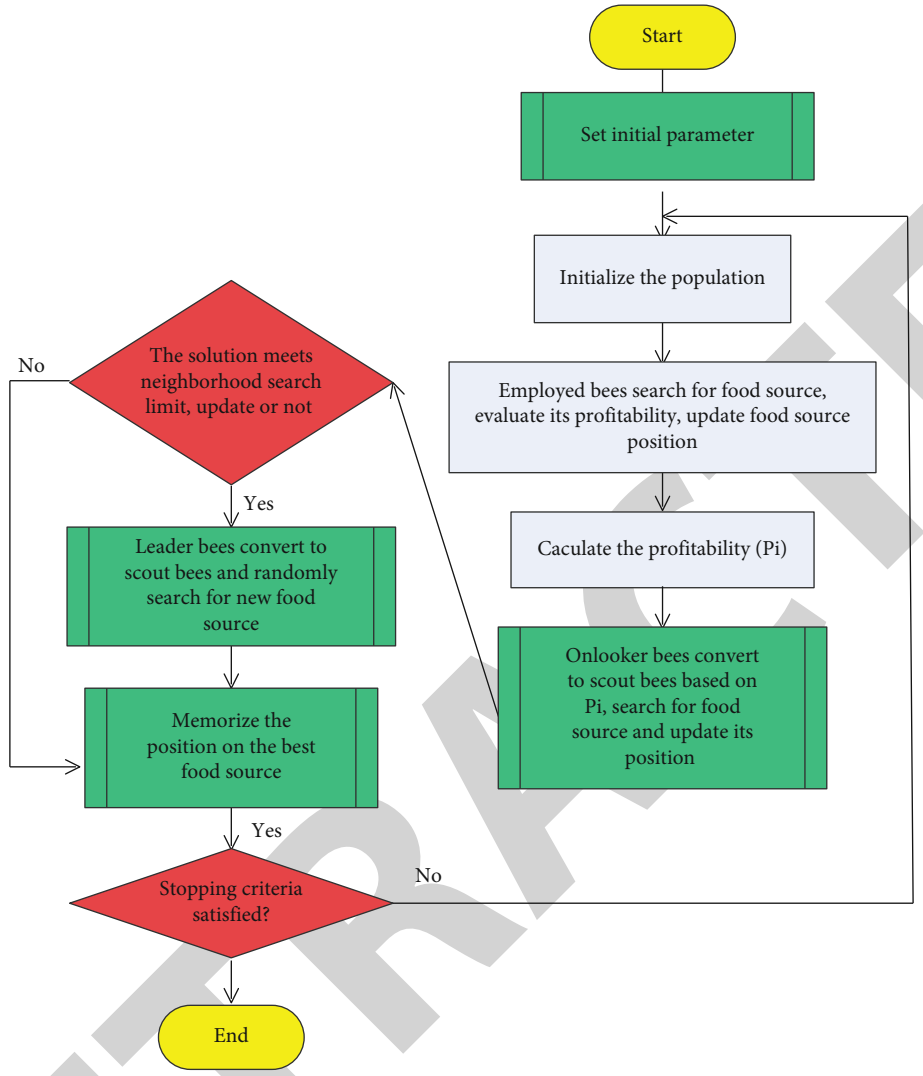

Figure 3: ABC algorithm flow chart.

$$x_{i,\text{new}}^{1j} = \begin{cases} x_i^{'j}, & \text{rand} < cr, \\ x_{\text{Global}}^{j} + \beta\left(x_{\text{Global}}^{j} - x_i^{'j}\right), & \text{rand} \geq cr. \end{cases} \quad (19)$$

By adjusting cr, the exploration ability and development ability of the algorithm can be adjusted. The experimental analysis shows that when the value of cr is about 0.6, the performance of the algorithm is better. The value of β is [−1, 1], which can effectively reduce the impact of this addition on the algorithm exploration ability.

Since the addition of the global optimal term limits the performance of the algorithm to a certain extent, the tabu table in the tabu search algorithm is added to speed up the search ability and optimization speed of the algorithm, and an improved TS-IABC algorithm based on tabu search is formed.

(1) The initial parameters are set, and the taboo table T is empty. The number of bee colonies is N, the maximum number of searches is Limit, the maximum number of iterations is MCN, and the initial solution generated by the global search is x_i ($x_i = 1, 2, \ldots, N$). The corresponding fitness function fiti can be calculated according to formula (16).

(2) The correlation data are sampled. The three-point estimation method calculates the probabilistic power flow, and the obtained fitness function value in each objective function value can be used for bee colony division. The larger fiti value is the lead bee, and the smaller fiti value is the observer bee.

(3) The lead bee performs a neighborhood search according to formula (18) and generates a new solution $x_{i,\text{new}}^{jj}$. According to the crossover operation of equation (15) and the optimal solution generated by iteration, combined with the greedy criterion, the old nectar source is abandoned, the solution with larger fiti in $x_{i,\text{new}}^{jj}$ and x_i^j is retained, and the tabu table is updated.

(4) Observer bees select nectar sources according to certain criteria, change their roles to lead bees, and search according to (3).

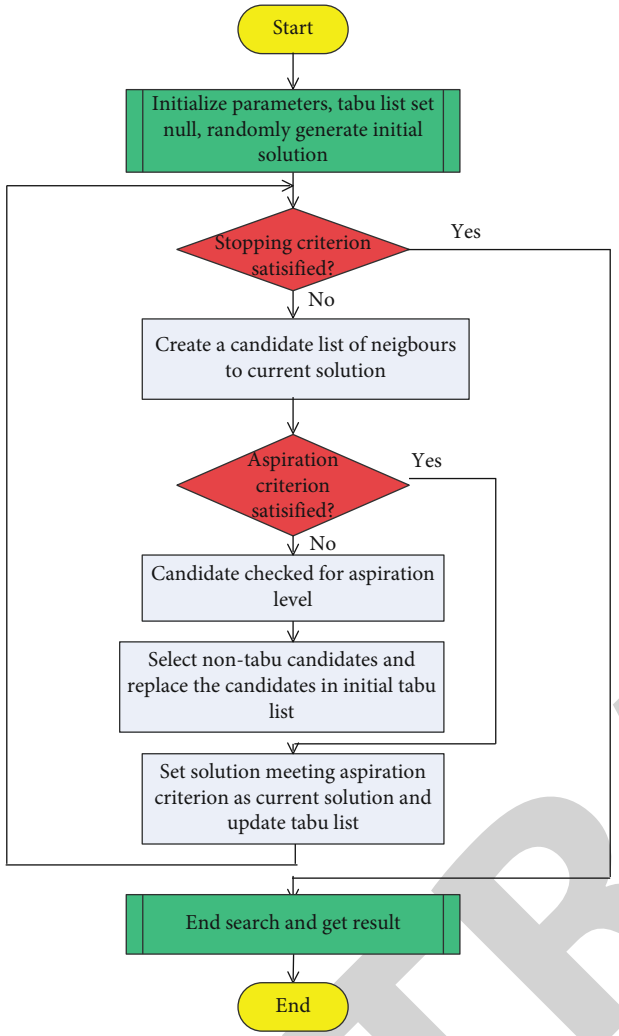

Figure 4: Flow chart of tabu search algorithm.

(5) The power flow calculation determines the local optimal solution and the global optimal solution. If no solution with higher fitness is found after reaching the number of local searches, the current solution is discarded, and it is recorded and updated to the tabu table. The lead bee or the observer bee will turn into a scout bee, generate a new solution according to equation (15), and judge whether the current solution is in the taboo list. If there is a record, the current solution is discarded and the search is repeated.

(6) One cycle is completed and the optimal solution is recorded.

(7) Whether the maximum number of iterations is satisfied is judged. If it is satisfied, the algorithm optimization ends and the result is output. Otherwise, it jumps to formula (2).

The process of improving the TS-IABC algorithm is shown in Figure 5.

Optimization problems often involve multiple optimization objectives, and multiple objectives may conflict in the optimization process, so that multiple objectives

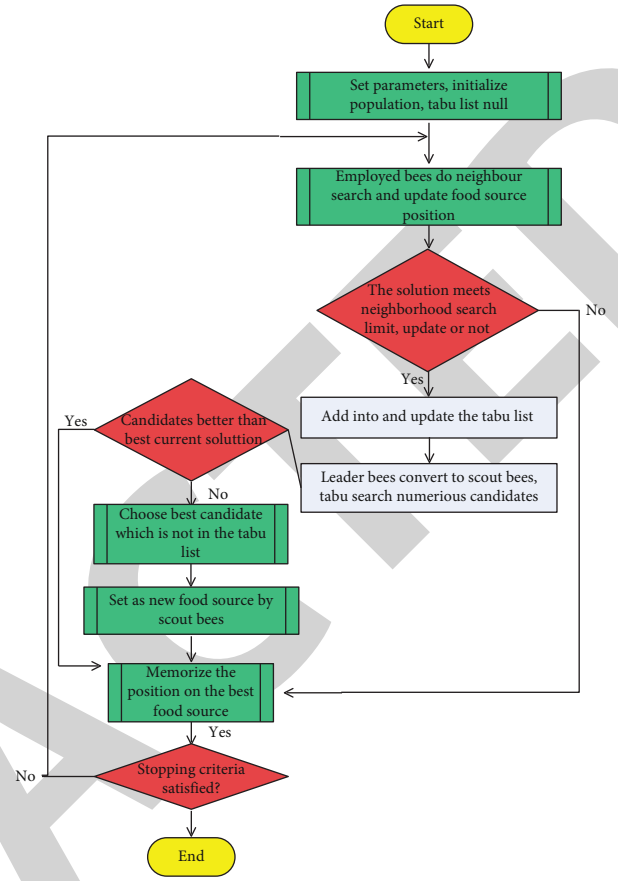

Figure 5: The process of improving the TS-IABC algorithm.

cannot be optimized at the same time. If the multi-objective is integrated and optimized through the weight coefficient, there is great unreasonableness. Therefore, this study uses the Pareto optimal theory to solve the multi-objective optimization problem of the distribution network with DG.

When multiple optimization objectives are involved at the same time, the objective function can be expressed as

$$\min F(x) = [f_1(X), f_2(X), \ldots, f_m(X)],$$
$$\text{s.t.} \quad \begin{cases} g_i(X) \le 0, & i = 1, 2, 3, \ldots, m\,(X \in S), \\ x_i^L \le x_i \le x_i^H, & i = 1, 2, \ldots, n. \end{cases} \tag{20}$$

In the formula, $X = (x_1, x_2, \ldots, x_m) \in S$ is the n-dimensional decision variable, S is the multi-objective optimization problem, and $f_m(X)$ is the mth objective function. At the same time, m is the total number of objective functions, $g_i(X)$ is the constraint condition, and x_i^L, x_i^H is the upper and lower limits of the variable x_i, respectively.

From the constraints in formula (21), we can get

$$\Omega = \left\{x | g_i(X) \le 0, \quad x_i^L \le x_i \le x_i^H\right\}. \tag{21}$$

Among them, the set Ω is the feasible region of S, and there is $\Omega \subseteq X$.

Figure 6 shows the relationship between the basic space, feasible solution set, and feasible region.

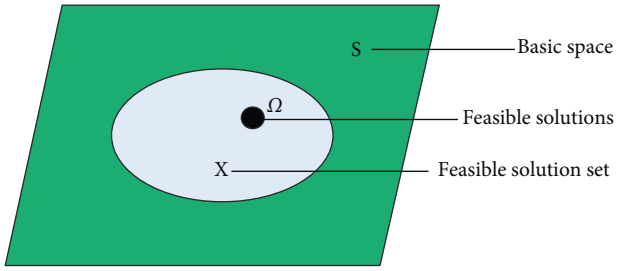

Figure 6: Relationship between basic space, feasible region, and feasible solution.

(1) *Pareto Control.* The two decision variables are X, $Y \in S$, and S is the solution space, which only satisfies

$$\begin{cases} \forall_i \in \{1, 2, \ldots, m\}, & f_i(X) \le f_i(Y), \\ \exists_i \in \{1, 2, \ldots, m\}, & f_i(X) < f_i(Y). \end{cases} \tag{22}$$

It can be said that X dominates Y, denoted as $X > Y$. At this point, X is nondominated and Y is dominated. If the conditions are not met, there is no dominance relationship.

(2) *Pareto Optimal Solution and Pareto Optimal Solution Set.* When there is $X \in S$ and there is no $X' \in S$ satisfying $X' > X$, it can be considered that the nondominant solution of S is X, and X at this time is the Pareto optimal solution. The optimal solution set contains all optimal solutions.

From the analysis of mathematical theory, the solutions contained in the optimal solution set are all optimal solutions with the same properties. If one wants to seek a set of top-level solutions in the solution set, it needs to be determined according to the preference of the decision maker.

(3) *Frontier of Pareto Optimal Solution.* Two objective functions $\min(F_1)$, $\min(F_2)$ are taken as examples, and $\{X^*\}$ is set as its Pareto nondominated solution set, then the Pareto frontier can be defined as

$$PF^* = \{F_1, F_2 | X \in \{X^*\}\}. \tag{23}$$

The essence of multi-objective optimization is to map from the search space to the target space. The optimal solution front can be considered as a subset of the target space. The optimal solution is a subset in the search space, and the optimal solutions together form a surface (line) in the search space.

The dual objective function (F_1, F_2) is taken as an example, and its Pareto frontier solution is a curve in the set, as shown in Figure 7.

The solid line and the dashed line together enclose the solution space of the two objective functions. The solid line is the Pareto frontier, the point abc, is the Pareto nondominated solution, and the points not on the Pareto frontier are the solutions dominated by the nondominated solution. If the problem involved has N objective functions, the solution space is an N-dimensional space surface.

There is only one optimal solution for a single objective function. However, each objective function in the multiobjective function has its own fitness function, and it is impossible to optimize all objective functions at the same time. Therefore, it is necessary to perform a compromise

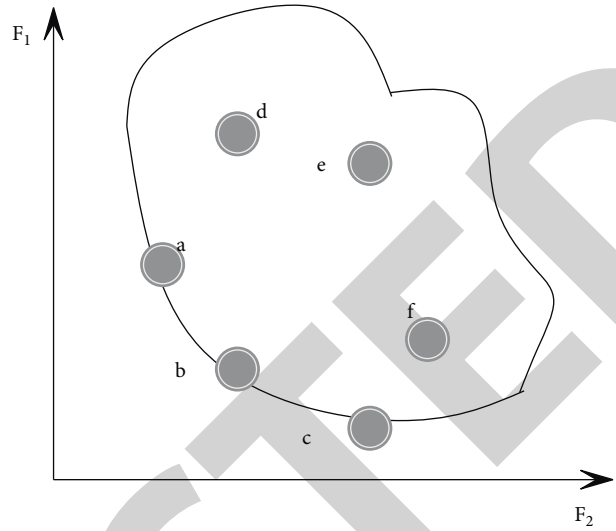

Figure 7: Pareto frontier for multiobjective optimization.

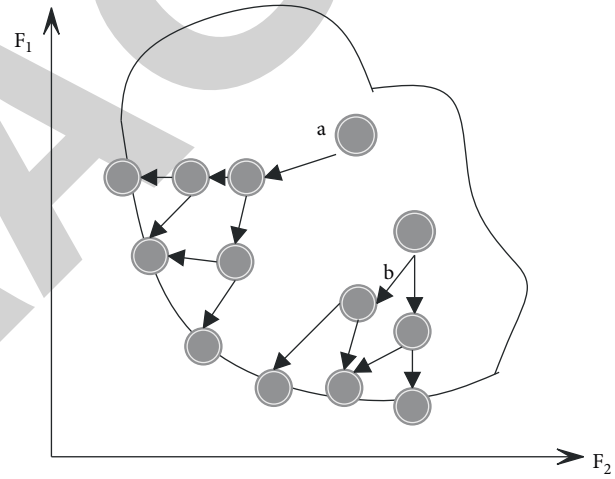

Figure 8: Population evolution direction.

process to find the optimal solution set—the Pareto optimal solution set, that is, to ensure that the population is close to the Pareto frontier, as shown in Figure 8.

3. Model Testing and Algorithm Analysis

3.1. Test Function. To test the TS-IABC algorithm, four standard functions are selected to conduct experiments to verify the algorithm's optimization ability. Table 1 presents the test functions and their associated data.

3.2. Experimental Verification and Result Analysis. In this study, TS algorithm, IABC algorithm, and TS-IABC algorithm are used to optimize the above four functions 20 times, and the function value of each optimization is recorded and the average value is calculated. Figure 9 shows a comparison diagram of the optimization effect of the algorithm.

Parameter setting: the total number of bee colonies N is 50, the maximum number of iterations MCN is 100, the maximum number of searches for a single nectar source

Table 1: Test function of improved artificial bee colony algorithm.

Function	Expression	Search range	Theoretical optimal solution
f_1 (Sphere)	$f(x) = \sum_{i=1}^{2} x_i^2$	$[-5.12, 5.12]$	$f(0) = 0$
f_2 (Rosenbrock)	$f(x, y) = 100(x^2 - y^2) + (1 - x)^2$	$[-2.048, 2.048]$	$f(1, 1) = 0$
f_3 (Rastrigin)	$f(x) = \sum_{i=1}^{D} [x_i^2 - 10 \cos \cos(2\pi x_i) + 10]$	$[-5.12, 5.12]$	$f(0, 0) = 1$
f_4 (griewank)	$f(x) = (1/4000) \sum_{i=1}^{D} x_i^2 - \prod_{i=1}^{D} \cos(x_2/\sqrt{i}) + 1$	$[-100, 100]$	$f(0) = 0$

In the table, f_1 and f_2 are single-level functions, and f_3 and f_4 are multi-level functions.

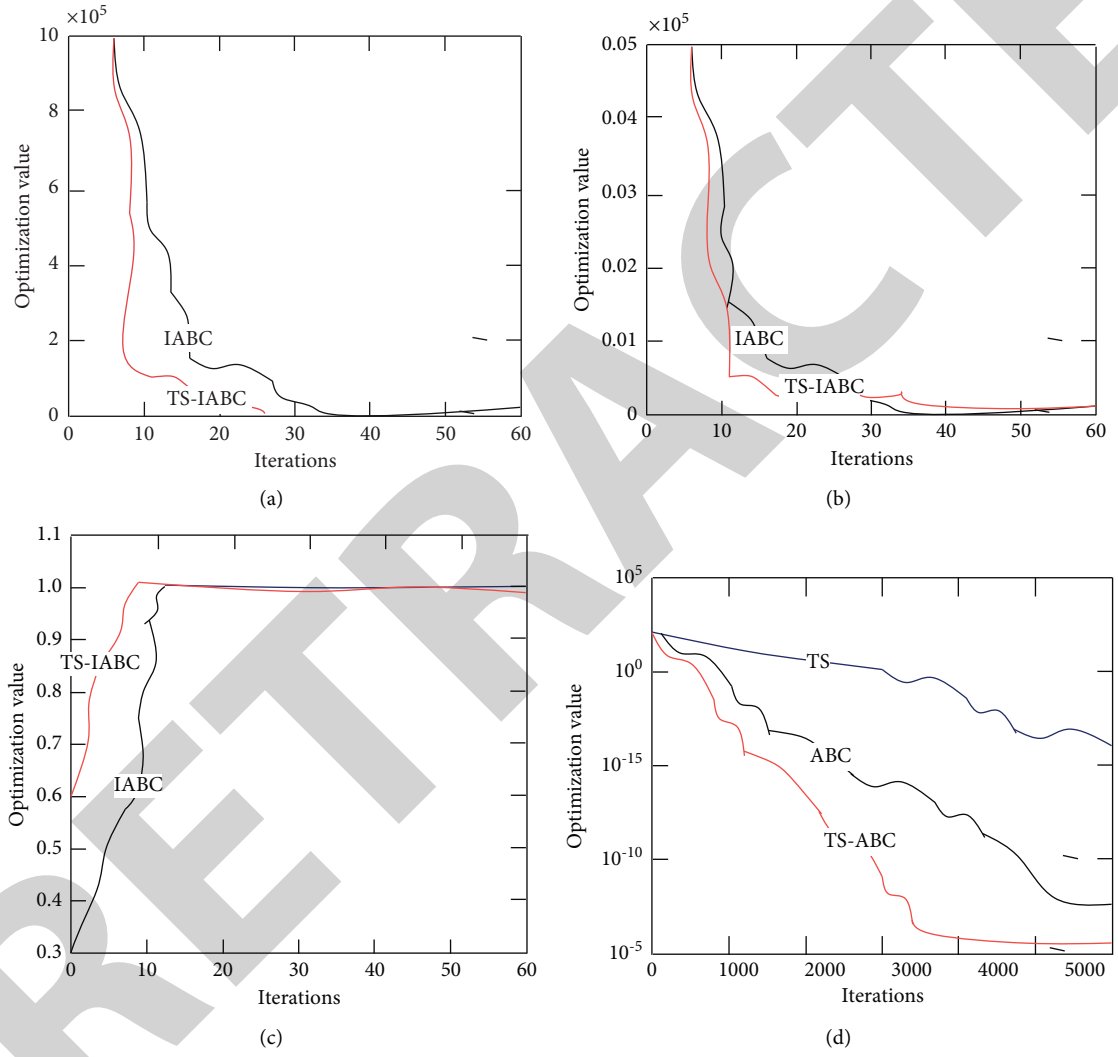

Figure 9: Optimization curve of the function. (a) Optimization curve of function f_1. (b) Optimization curve of function f_2. (c) Optimization curve of function f_3. (d) Optimization curve of the function f_4.

Limit is 30, the number of candidate solutions in the TS algorithm is Num = 80, and the number of candidate solutions in the TA-IABC algorithm is Num = 20.

It can be seen from the comparison chart of algorithm effects that compared with the other two algorithms, the improved TS-IABC algorithm has stronger search ability, faster optimization speed, higher calculation accuracy, and can better balance the local optimum and the global optimum. On the basis of the above, the optimal intelligent distribution method of the distribution network in the presence of distributed power generation proposed in this study is evaluated, and the results shown in Table 2 are obtained.

From the above research, it can be seen that the optimal intelligent distribution method of the distribution network in the presence of distributed power generation proposed in

Table 2: Verification of the effect of optimal intelligent distribution method of distribution network in the presence of distributed power generation.

Num	Distribution network	Num	Distribution network
1	89.73	17	86.21
2	90.50	18	88.93
3	85.87	19	87.89
4	86.38	20	86.90
5	89.61	21	88.45
6	84.44	22	85.09
7	90.64	23	91.22
8	84.30	24	90.18
9	85.05	25	89.94
10	88.53	26	89.41
11	84.67	27	87.20
12	88.76	28	91.51
13	86.47	29	89.56
14	90.75	30	90.54
15	91.32	31	88.52
16	86.65	32	87.37

this study has good results, and can effectively promote the intelligent distribution of distribution network.

4. Conclusion

The size of the distribution network loss is mainly affected by the system power flow. With the grid-connected operation of distributed power generation, the branch power flow in the distribution network is no longer simply flowing in one direction. That is, the flow direction of the branch power flow may become very complicated, and even reverse power flow may occur, resulting in changes in the system network loss. Under normal circumstances, the access to distributed power sources will reduce the transmission energy on the transmission line, thereby reducing the loss of the distribution network. However, in fact, the increase or decrease of network loss is mainly determined by the grid connection of distributed power sources. This study combines the intelligent algorithm to carry out the optimization of intelligent distribution analysis of the distribution network based on distributed power generation, so as to improve the intelligent analysis and reconstruction effect of the distribution network. The simulation results show that the optimal intelligent distribution method of the distribution network in the presence of distributed power generation proposed in this study has a good effect and can promote the optimal intelligent distribution of the distribution network.

Data Availability

The labeled dataset used to support the findings of this study is available from the corresponding author upon request.

Conflicts of Interest

The authors declare that there are no conflicts of interest.

References

[1] J. Zhu, H. Hu, Z. He, X. Guo, and W. Pan, "A power-quality monitoring and assessment system for high-speed railways based on train-network-data center integration," *Railway Engineering Science*, vol. 29, no. 1, pp. 30–41, 2021.

[2] B. Qu, N. Li, Y. Liu, and F. E. Alsaadi, "Estimation for power quality disturbances with multiplicative noises and correlated noises: a recursive estimation approach," *International Journal of Systems Science*, vol. 51, no. 7, pp. 1200–1217, 2020.

[3] F. Xiao and Q. Ai, "Data-driven multi-hidden Markov model-based power quality disturbance prediction that incorporates weather conditions," *IEEE Transactions on Power Systems*, vol. 34, no. 1, pp. 402–412, 2019.

[4] W. Qiu, Q. Tang, J. Liu, and W. Yao, "An automatic identification framework for complex power quality disturbances based on multifusion convolutional neural network," *IEEE Transactions on Industrial Informatics*, vol. 16, no. 5, pp. 3233–3241, 2020.

[5] S. A. Kumar and D. Chandramohan, "Fault test analysis in transmission lines throughout interfering synchrophasor signals," *ICT Express*, vol. 5, no. 4, pp. 266–270, 2019.

[6] F. Z. Dekhandji, S. Talhaoui, and Y. Arkab, "Power quality detection, classification and monitoring using LABVIEW," *Algerian Journal of Signals and Systems*, vol. 4, no. 2, pp. 101–111, 2019.

[7] W. Qiu, Q. Tang, K. Zhu, W. Wang, Y. Liu, and W. Yao, "Detection of synchrophasor false data injection attack using feature interactive network," *IEEE Transactions on Smart Grid*, vol. 12, no. 1, pp. 659–670, 2021.

[8] A. Sundararajan, T. Khan, A. Moghadasi, and A. I. Sarwat, "Survey on synchrophasor data quality and cybersecurity challenges, and evaluation of their interdependencies," *Journal of Modern Power Systems and Clean Energy*, vol. 7, no. 3, pp. 449–467, 2019.

[9] A. Khair, M. Zuhaib, and M. Rihan, "Effective utilization of limited channel PMUs for islanding detection in a solar PV integrated distribution system," *Journal of the Institution of Engineers: Serie Bibliographique*, vol. 102, no. 1, pp. 75–86, 2021.

[10] M. Asadi, M. N. Harikandeh, and M. Hamzenia, "Detecting and locating power quality issues by implementing wavelet transform," *International Journal of Science and Engineering Applications*, vol. 10, no. 07, pp. 96–100, 2021.

[11] W. Wang, C. Chen, W. Yao, K. Sun, W. Qiu, and Y. Liu, "Synchrophasor data compression under disturbance conditions via cross-entropy-based singular value decomposition," *IEEE Transactions on Industrial Informatics*, vol. 17, no. 4, pp. 2716–2726, 2021.

[12] S. Vlahinić, D. Franković, B. Juriša, and Z. Zbunjak, "Back up protection scheme for high impedance faults detection in transmission systems based on synchrophasor measurements," *IEEE Transactions on Smart Grid*, vol. 12, no. 2, pp. 1736–1746, 2021.

[13] B. K. Panigrahi, A. Bhuyan, J. Shukla, P. K. Ray, and S. Pati, "A comprehensive review on intelligent islanding detection techniques for renewable energy integrated power system," *International Journal of Energy Research*, vol. 45, no. 10, pp. 14085–14116, 2021.

[14] P. K. Ganivada and P. Jena, "Frequency disturbance triggered d-axis current injection scheme for islanding detection," *IEEE Transactions on Smart Grid*, vol. 11, no. 6, pp. 4587–4603, 2020.

[15] X. Xie, Y. Zhan, H. Liu, and C. Liu, "Improved synchrophasor measurement to capture sub/super-synchronous dynamics in power systems with renewable generation," *IET Renewable Power Generation*, vol. 13, no. 1, pp. 49–56, 2019.

[16] E. M. Molla, C. H. Liu, and C. C. Kuo, "Power quality improvement using microsystem technology for wind power plant," *Microsystem Technologies*, vol. 26, no. 6, pp. 1799–1811, 2020.

[17] R. M. Radhakrishnan, A. Sankar, and S. Rajan, "Synchrophasor based islanding detection for microgrids using moving window principal component analysis and extended mathematical morphology," *IET Renewable Power Generation*, vol. 14, no. 12, pp. 2089–2099, 2020.

[18] Y. Hao, M. Wang, J. H. Chow, E. Farantatos, and M. Patel, "Modelless data quality improvement of streaming synchrophasor measurements by exploiting the low-rank Hankel structure," *IEEE Transactions on Power Systems*, vol. 33, no. 6, pp. 6966–6977, 2018.

[19] W. Qiu, Q. Tang, Y. Wang, L. Zhan, Y. Liu, and W. Yao, "Multi-view convolutional neural network for data spoofing cyber-attack detection in distribution synchrophasors," *IEEE Transactions on Smart Grid*, vol. 11, no. 4, pp. 3457–3468, 2020.

[20] A. Sankar, A. Sankar, and S. R, "Synchrophasor data driven islanding detection, localization and prediction for microgrid using energy operator," *IEEE Transactions on Power Systems*, vol. 36, no. 5, pp. 4052–4065, 2021.

[21] R. Pal and S. Gupta, "Topologies and control strategies implicated in dynamic voltage restorer (DVR) for power quality improvement," *Iranian Journal of Science and Technology, Transactions of Electrical Engineering*, vol. 44, no. 2, pp. 581–603, 2020.